Journal of Engineering Physics and Thermophysics, Vol. 77, No. 3, 2004

IDENTIFICATION OF HEAT-EXCHANGE PROCESSES IN A SUPERSONIC SPATIAL FLOW PAST AIRCRAFT

A. Ya. Kuzin

UDC 536.24.01

Direct and inverse problems of heat exchange in a supersonic spatial flow past the front part of an aircraft in the form of a spherically blunted nose cone have been solved numerically. The prospects of using high-heat-conductivity materials and the blowing of the gas-coolant for lowering the temperature on the surface of an aerodynamic body have been shown. A comparison of the solutions of the direct and inverse problems in one-, two-, and three-dimensional formulations for various materials of the sheath has been made. The error in recovering the heat flow by the thin-walled method has been estimated.

Under the interaction of high-enthalpy gas flows with aircraft (AC), one of the most complicated problems is the thermal protection of their structures. To solve it, both passive and active methods of thermal protection and combined methods based on blowing of the gas-coolant into a high-enthalpy gas flow from porous structural elements with a simultaneous heat flow on the surface due to the choice of the high-heat-conductivity material of the composite sheath [1–6] are used. To investigate and substantiate them, along with the methods for solving direct problems (DP) [1–3], methods for solving inverse problems (IP) are used [4–6]. Because of the extreme operating conditions of the structures, lack of information about the processes being investigated, and the increasing requirements on accuracy of determination of the heat-exchange characteristics on the surface of aerodynamic bodies, the application of the latter in wide ranges of change in the process time and properties of the material is becoming particularly urgent [7].

To solve multidimensional boundary IPs, the iteration regularization method has proved to be good [8, 9]. For mathematical models of the mechanics of reacting media, this method complements the regularized numerical methods well [10]. In [5, 6], the latter were successfully used to solve three-dimensional boundary IPs of a supersonic spatial flow. The use of three-dimensional formulations in these problems is necessitated by the fact that as an aircraft moves at the angle of attack, the heat flows on its front part not only along the longitudinal but also along the circular coordinate due to the wide difference between the thermal flows on the windward and leeward sides. Blowing of the gas-coolant promotes a decrease in the temperature in the region of the porous spherical dulling, and the use of high-heat-conductivity materials leads to a heat flow from the peripheral part of the cone into the porous nose [3, 4, 6]. The separate and combined influence of these processes in the spatial case on the recovered temperature and thermal flow in wide ranges of change in the thermophysical characteristics of the sheath material and the process time requires a detailed study and substantiation. Of undoubted interest is also the estimation of the validity range of the simpler one- and two-dimensional algorithms of solving direct and inverse heat-exchange problems and the widely used thin-wall method for determining the heat flow at the boundary of an aerodynamic body.

In the present paper, using the complete mathematical formulation of the problem on heating of a spherically blunted nose cone and the developed algorithms for solving three-dimensional and inverse problems from [5, 6], we have investigated the influence of the heat flow along the longitudinal and circular coordinates and the blowing of the gas-coolant on the heat-exchange characteristics in a wide range of change in the thermophysical characteristics of the sheath material. The error in solving direct and inverse problems on the basis of one-, two-, and three-dimensional mathematical models has been found. The possibility of using the thin-wall method to recover the thermal flow at the interface has been analyzed.

Physical and Mathematical Formulation of the Direct and Inverse Problems. We consider the heating of an equidistant composite sheath of a spherically blunted nose cone flown at the angle of attack by a supersonic air

Tomsk State University; email: kuzin@niipmm.tsi.tomsk.su. Translated from Inzhenerno-Fizicheskii Zhurnal, Vol. 77, No. 3, pp. 165–173, May–June, 2004. Original article submitted January 15, 2003; revision submitted March 24, 2003.

1062-0125/04/7703-0663

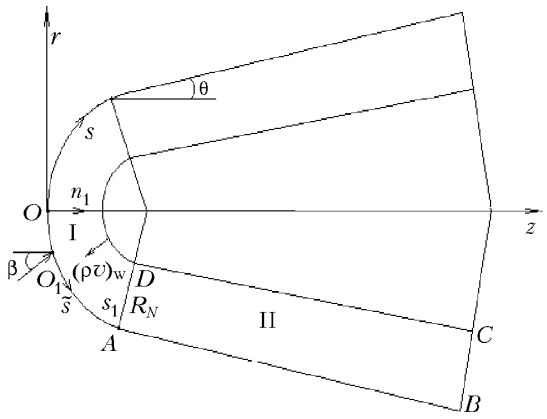

Fig. 1. Scheme of heating of the composite sheath in the $\eta = 0$, $\eta = \pi$ symmetry planes.

flow (Fig. 1). The heat-and-mass transfer process in a sheath consisting of a penetrable spherical part and an impenetrable conical part with allowance for the assumptions that the filtration process of the blown gas in the direction of the normal to the surface is one-dimensional and the porous medium in the natural coordinate system connected with the surface of the body with the origin of coordinates at the frontal critical point 0 has one temperature is described by the energy equation for the porous spherical dulling (Fig. 1, region I)

$$c_{p\Sigma}\frac{\partial T_1}{\partial t} - c_{pg}\frac{(\rho v)_{\rm w} r_{1\rm w}}{Hr_1}\frac{\partial T_1}{\partial n_1} = \frac{1}{Hr_1}\left[\frac{\partial}{\partial n_1}\left(Hr_1\lambda_\Sigma\frac{\partial T_1}{\partial n_1}\right) + \frac{\partial}{\partial s}\left(\frac{r_1\lambda_\Sigma}{H}\frac{\partial T_1}{\partial s}\right) + \frac{\partial}{\partial \eta}\left(\frac{H}{r_1}\lambda_\Sigma\frac{\partial T_1}{\partial \eta}\right)\right], \quad 0 < s < s_A, \tag{1}$$

and the heat-conduction equation for the conical part of the sheath (Fig. 1, region II)

$$(r\rho c_p)_2\frac{\partial T_2}{\partial t} = \frac{\partial}{\partial n_1}\left(r_2\lambda_2\frac{\partial T_2}{\partial n_1}\right) + \frac{\partial}{\partial s}\left(r_2\lambda_2\frac{\partial T_2}{\partial s}\right) + \frac{1}{r_2}\frac{\partial}{\partial \eta}\left(\lambda_2\frac{\partial T_2}{\partial \eta}\right), \quad s_A < s < s_B, \quad 0 < n_1 < L, \quad 0 < \eta < \pi,$$
$$0 < t \le t_{\rm fin}, \tag{2}$$

with the corresponding initial and boundary conditions

$$T_i\big|_{t=0} = T_{\rm in}, \quad i = 1, 2; \tag{3}$$

$$q_{\rm w} - \varepsilon_1\sigma T_{1\rm w}^4 = -\lambda_\Sigma\,(\partial T_1/\partial n_1)\big|_{\rm w}, \quad 0 \le s < s_A; \tag{4}$$

$$q_{\rm w} - \varepsilon_2\sigma T_{2\rm w}^4 = -\lambda_2\,(\partial T_2/\partial n_1)\big|_{\rm w}, \quad s_A \le s \le s_B; \tag{5}$$

$$\lambda_\Sigma\left(\frac{\partial T_1}{\partial n_1}\right)\Big|_{\rm ins} = \frac{r_{1\rm w}c_{pg}\,(\rho v)_{\rm w}}{(Hr_1)_{\rm ins}}\,(T_{\rm in} - T\big|_{\rm ins}), \quad 0 \le s < s_D; \tag{6}$$

$$\left.\frac{\partial T_2}{\partial n_1}\right|_{\rm ins} = 0, \quad s_D \le s \le s_C; \tag{7}$$

$$\frac{\lambda_\Sigma}{H}\frac{\partial T_1}{\partial s} = \lambda_2\frac{\partial T_2}{\partial s}, \quad T_1 = T_2 - \text{on the conjunction ring } AD; \tag{8}$$

$$\frac{\partial T_2}{\partial s} = 0 - \text{on the line } BC\,; \tag{9}$$

$$\left.\frac{\partial T_i}{\partial \eta}\right|_{\eta=0} = \left.\frac{\partial T_i}{\partial \eta}\right|_{\eta=\pi}, \quad i = 1, 2 - \text{in the symmetry plane}\,; \tag{10}$$

$$\bar{s} = s/R_N\,, \quad H = (R_N - n_1)/R_N\,, \quad r_1 = (R_N - n_1)\sin\bar{s}\,,$$

$$r_2 = (R_N - n_1)\cos\theta + (s - s_A)\sin\theta\,, \quad s = s_A + \cos^{-1}\theta\,[z + (\sin\theta - 1)\,R_N]\,.$$

In determining the temperature $T(n_1, s, \eta, t)$ in the composite sheath from the DP solution, the heat flow from the gaseous phase q_w is given by the formulas from [11] for the spatial laminar and turbulent flow conditions in the boundary layer. The decay of the heat flow due to the blowing of the gas-coolant having the same composition as the free air stream is taken into account by the formulas from [12]. As a result, in the coordinate system connected with the stagnation point O_1 on the porous spherical part for the laminar flow conditions in the boundary layer we have

$$q_\text{w} = \left(\frac{\alpha}{c_p}\right)^{(0)}\left[1 - \frac{0.6\,(\rho v)_\text{w}}{(\alpha/c_p)^{(0)}}\right](h_\text{r} - h_\text{w})\,, \tag{11}$$

$$\left(\frac{\alpha}{c_p}\right)^{(0)} = \frac{1.05 V_\infty^{1.08}\,[0.55 + 0.45\cos(2\tilde{s})]}{(R_N/\rho_\infty)^{0.5}}\,, \tag{12}$$

$$h_\text{r} = h_{\text{e}0}\left[\left(\frac{p_\text{e}}{p_{\text{e}0}}\right)^{(\gamma-1)/\gamma} + \left(\frac{u_\text{e}}{v_\text{m}}\right)^2 \text{Pr}^{0.5}\right], \quad 0 \le \tilde{s} \le \tilde{s}_*\,; \tag{13}$$

for the turbulent flow conditions

$$q_\text{w} = \left(\frac{\alpha}{c_p}\right)^{(0)} \exp\left[-\frac{0.37\,(\rho v)_\text{w}}{(\alpha/c_p)^{(0)}}\right](h_\text{r} - h_\text{w})\,, \tag{14}$$

where

$$\left(\frac{\alpha}{c_p}\right)^{(0)} = \frac{16.4 V_\infty^{1.25}\,\rho_\infty^{0.8}}{R_N^{0.2}\,(1 + h_\text{w}/h_{\text{e}0})^{2/3}}\,(3.75\sin\tilde{s} - 3.5\sin^2\tilde{s})\,; \tag{15}$$

$$h_\text{r} = h_{\text{e}0}\left[\left(\frac{p_\text{e}}{p_{\text{e}0}}\right)^{(\gamma-1)/\gamma} + \left(\frac{u_\text{e}}{v_\text{m}}\right)^2 \text{Pr}^{1/3}\right]; \quad \tilde{s}_* < \tilde{s} < \tilde{s}_1\,; \tag{16}$$

$$\frac{u_\text{e}}{v_\text{m}} = \left[1 - \left(\frac{p_\text{e}}{p_{\text{e}0}}\right)^{(\gamma-1)/\gamma}\right]^{0.5}; \quad h_{\text{e}0} = h_\infty\,[1 + 0.5\,(\gamma - 1)\,\text{M}_\infty^2]\,; \quad h_\text{w} = b_1 T_\text{w} + b_2 T_\text{w}^2/2\,;$$

$$v_\text{m} = (2h_{\text{e}0})^{0.5}\,; \quad \tilde{s} = \arccos(\cos\bar{s}\cos\beta + \sin\bar{s}\sin\beta\cos\eta)\,.$$

The heat flow in the screening zone with allowance for the blowing is defined by the formula [2, 13]

$$q_{\mathrm{w}} = \left(\frac{\alpha}{c_p}\right)^{(0)} (1 - \zeta_1 b^{\zeta_2}) (h_{\mathrm{r}} - h_{\mathrm{w}}) . \tag{17}$$

Here

$$\left(\frac{\alpha}{c_p}\right)^{(0)} = \frac{16.4 V_\infty^{1.25} \rho_\infty^{0.8}\, 2.2\, (p_{\mathrm{e}}/p_{\mathrm{e0}})\, (u_{\mathrm{e}}/v_{\mathrm{m}})}{R_N^{0.2} (1 + h_{\mathrm{w}}/h_{\mathrm{e0}})^{2/3} k^{0.4} r_{2\mathrm{w}}^{-0.2}}; \quad k = \frac{\gamma - 1 + 2/\mathrm{M}_\infty^2}{\gamma + 1}; \quad \bar{r}_{2\mathrm{w}} = \frac{r_{2\mathrm{w}}}{R_N}; \quad \tilde{s}_A \le \tilde{s} \le \tilde{s}_B .$$

For the flow rate of the gas-coolant according to the law $(\rho v)_{\mathrm{w}}(\tilde{s}) = (\rho v)_{\mathrm{w}}(0)(1 + a \sin^2 \tilde{s})$ we have [2]

$$b = \frac{2 (\rho v)_{\mathrm{w}} (0) \left\{1 - \cos \tilde{s}_1 + a\, [2/3 - \cos \tilde{s}_1 + (1/3) \cos^3 \tilde{s}_1]\right\}}{(\alpha/c_p)^{(0)} (\bar{s} - \bar{s}_1)\, [2 \cos \theta + (\bar{s} - \bar{s}_1) \sin \theta]},$$

$$\cos \tilde{s}_1 = \cos \bar{s}_1 \cos \beta + \sin \bar{s}_1 \sin \beta \cos \eta , \quad \bar{s}_1 = \bar{s}_A = \pi/2 - \theta .$$

In solving the three-dimensional IP, the temperature $T_{\mathrm{w}}(s, \eta, t)$, the convective stream $q_{\mathrm{w}}(s, \eta, t)$, and the total $Q_{\mathrm{w}}(s, \eta, t) = q_{\mathrm{w}}(s, \eta, t) - \varepsilon\sigma T_{\mathrm{w}}^4$ heat fluxes at the boundary are determined on the basis of the mathematical model (1)–(3), (6)–(10) and the given temperature on the back of the sheath

$$T(L, s, \eta, t) = T_{\mathrm{ins}}^{\mathrm{exp}}(s, \eta, t) . \tag{18}$$

Algorithms for Solving the Direct and Inverse Problems. In solving three-dimensional DPs and IPs, the algorithms from [5, 6] based on the method of splitting in spatial variables n_1, s, and η were used [14]. In the direct problem, the one-dimensional energy and heat-conduction equations obtained as a result of the splitting on each time layer were calculated with a variable step by the iteration-interpolation method (IIM) [15] with iterations over coefficients with a given accuracy. The temperature in the direction was calculated throughout, beginning with the windward side and ending with the leeward one with the fulfillment at the point $s = 0$ of the "matching" conditions (equality of temperatures and heat flows), since when the body is moving at a nonzero angle of attack the symmetry condition at the point $s = 0$ is no longer fulfilled. As a result, to calculate the sheath temperature, it is enough to vary the circular coordinate from 0 to $\pi/2$. For other values of η the temperature was determined from the symmetry condition at $\eta = 0$ and $\eta = \pi$, which reduced the counting time of the problem by one-half. The systems of difference equations for temperature determination in the directions of n_1, s, and η obtained by the IIM logical scheme were solved by the methods of nonmonotonic (in the direction of n_1 and s) and cyclic (in the direction of η) runs [16].

In the three-dimensional IP, upon application of the splitting method on each time layer the temperature in the direction of n_1 was calculated by the method of solving the one-dimensional IP from [5] on the basis of the known temperature $T_{\mathrm{ins}}^{\mathrm{exp}}(s, \eta, t)$, and in the directions of s and η — by the IIM. The temperature obtained on the previous time layer was used as the initial temperature for calculating the temperature on the next layer, and so on. By the found temperature field the total thermal flux $Q_{\mathrm{w}}(s, \eta, t)$ was found, and then from the boundary conditions (4) and (5) the convective thermal flow $q_{\mathrm{w}}(s, \eta, t)$ was found. The advantage of the applied method of solving the three-dimensional IP is that it permits investigating both fast and slow heat-exchange processes. Stability of the IP solution was attained due to the application of the implicit difference scheme of the IIM, which is closely related to the theory of splines, and the smoothing of the initial temperature $T_{\mathrm{ins}}^{\mathrm{exp}}(s, \eta, t)$ by either A. N. Tikhonov's regularization method [17] or cubic spline-functions, including two-dimensional ones [18]. If required, solution regularization in the directions of s and η by the method of [17] was used. The applied methods of solution instability suppression proved to be good in solving various one-dimensional [10] and two- and three-dimensional IPs [4–6].

Results of the Numerical Calculations. Numerical calculations of three-dimensional DPs and IPs were carried out on a Pentium-3 PC by programs developed in Fortran. The time of solving the reference three-dimensional

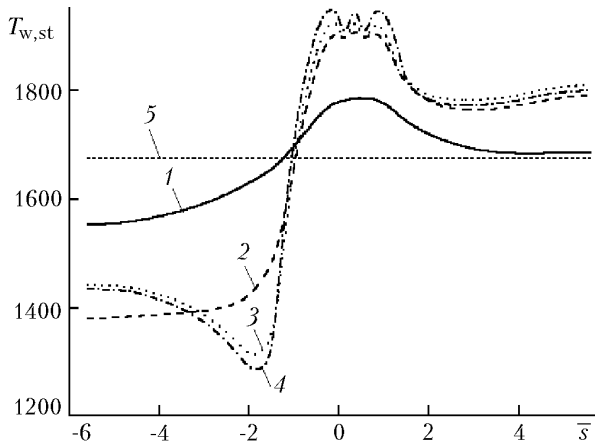

Fig. 2. $T_{w,st}$ distributions over $\bar{s}$: 1) for the copper sheath; 2) for the steel sheath; 3) for the carbon-filled plastic sheath; 4) $T_{w,eq}(\bar{s})$; 5) $T_{w,st}(\bar{s})$ at $\lambda \to \infty$. $T_{w,st}$, K.

variants of the direct and inverse problems up to the stationary temperature distribution (t = 200 sec) on a 11 × 41 × 13 computational mesh was ≈9 min. The direct and inverse problems were tested at the level of both individual program modules and programs as a whole. The main modules such as the solution of a one-dimensional parabolic equation of the general form with the most general boundary conditions and the solution of a one-dimensional boundary IP for this equation were checked on the known solutions [15, 19]. Testing of the spatial DP in a particular case as $t \to \infty$ without taking into account the heat flow on s and η was carried out by comparing the stationary temperature of the surface $T_{w,st}$ with the radiation equilibrium temperature $T_{w,eq}$. As tests, the numerical solutions from [3, 6] were also used. Testing of the spatial IP was carried out by comparison with the "exact" solution, as which the numerical solution of the spatial DP acted.

In the boundary layer, the laminar regime of the flow on a porous spherical sheath in the vicinity of the stagnation point and the turbulent regime on the remaining part of the spherical sheath and on the cone were considered. We used the popular model of the point laminary–turbulent transition in which the transition point $\tilde{s}_*$ was determined from the condition of the change of the difference sign of values (α/c_p) for the laminar (12) and turbulent (15) flows in the $[0, \bar{s}_1]$ range and depended on the parameters in formulas (12) and (15).

Serial calculations were performed for the diagnostic variables from [3, 6]: $c_{p\Sigma} = c_{p1}\rho_1(1-\varphi) + c_{pg}\rho_g\varphi$, $\lambda_\Sigma = \lambda_1(1-\varphi) + \lambda_g\varphi$, $c_{pg} = b_1 + b_2 T$, b_1 = 965.5, b_2 = 0.147, $T_{in} = T_\infty$ = 300 K, $c_{p\infty} = 10^3$ J/(kg·K), ρ_g = 1.3 kg/m^3, λ_g = 0.026 W/(m·K), L = 0.005 m, ε_i = 0.85 (i = 1, 2), R_N = 0.0185 m, ρ_∞ = 0.208 kg/m^3, V_∞ = 2080 m/sec, β = 20°, $\Theta = 5°$, φ = 0.34, γ = 1.4, M_∞ = 6, Pr = 0.72, ζ_1 = 0.285, ζ_2 = 0.165, and a = 0. As a sheath material, we considered a high-heat-conductivity material (copper, λ = 386 W/(m·K), ρ = 8950 kg/m^3, c_p = 376 J/(kg·K), a low-heat-conductivity material (carbon-filled plastic, λ = 0.75 W/(m·K), ρ = 1350 kg/m^3, c_p = 1062 J/(kg·K)), and a material with intermediate values of the thermophysical characteristics (steel, λ = 20 W/(m·K), ρ = 7800 kg/m^3, c_p = 600 J/(kg·K)). The pressure distribution on the body surface p_e/p_{e0} was found from the solution of the spatial gas-dynamic problem [20]. Figures 1–5 show the results of solving the direct and inverse problems with no allowance for the blowing, and Figures 6–9 show them with allowance for the blowing $(\rho v)_w$ = 1.626 kg/(m^2·sec) in the symmetry planes of η = 0 and η = π (except for Fig. 8, where the solution results are given in the planes of η = $\pi/2$ and $3\pi/2$).

Figure 2 shows the distributions of the stationary temperature of the surface $T_{w,st}$ (t = 200 sec) over the $\bar{s}$ coordinate on the windward $(\bar{s} > \bar{s}_{O_1})$ and leeward $(\bar{s} < 0)$ U $(0 < \bar{s} < \bar{s}_{O_1})$ sides for sheaths from different materials. The radiation equilibrium temperature $T_{w,eq}$ was found from the energy equations on the spherical and conical surfaces:

$$q_w - \varepsilon_i \sigma T_{w,eq}^4 = 0 \,. \tag{19}$$

It determines the maximum attainable temperature of the surface in the absence of heat flow in the longitudinal and circular directions. As would be expected, the strongest effect of the heat flow is observed in the copper sheath and the weakest effect — in the carbon-filled plastic sheath. For the latter, the stationary surface temperature differs from

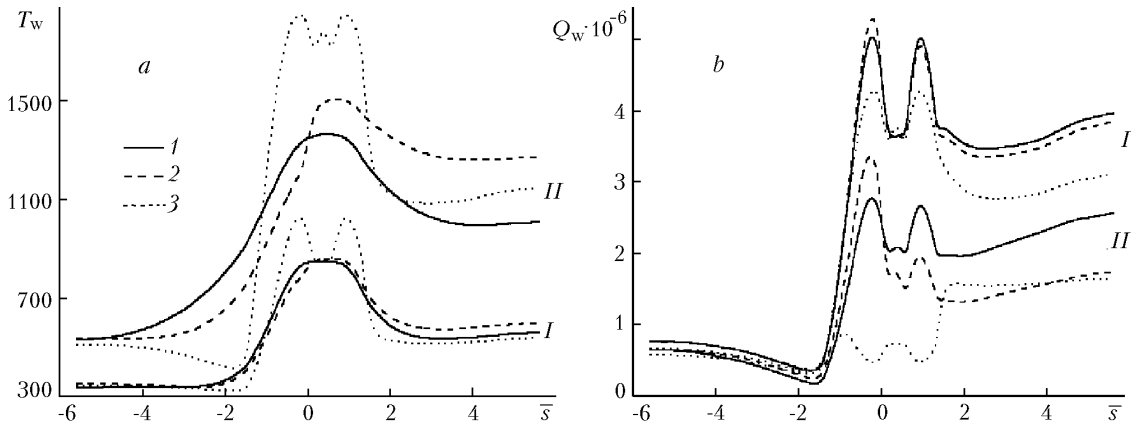

Fig. 3. Dependences of T_w (a) and Q_w (b) on $\bar{s}$ for the copper sheath at t = 1 sec (groups of curves I) and 5 sec (groups of curves II) obtained from the solution of the three-dimensional (1), two-dimensional (2), and one-dimensional (3) DPs. T_w, K; Q_w, W/m^2.

the radiation equilibrium temperature only slightly, since the heating process for it is close to the one-dimensional one. As a result of the heat flow along the longitudinal and circular coordinates, $T_{w,st}$ for the copper sheath is much higher than $T_{w,eq}$ on the leeward side and more than 100 K lower on the windward side. For the steel sheath the difference between these temperatures begins to show up appreciably only on the leeward side and is insignificant on the windward side. The results of the calculation of the steady-state regime of the process as $\lambda_i \to \infty$ (i = 1, 2) show that flattening of the temperature profile in the aerodynamic material occurs. The highest value of the stationary surface temperature for all considered materials is observed in the region of the peak thermal flux for the turbulent regime in the boundary layer near the stagnation point.

Figure 3 illustrates the illegitimacy of using one-dimensional and two-dimensional formulations in solving DPs for high-heat-conductivity materials of the type of copper. Here curves 1 were obtained with allowance for the heat transfer in the directions of n_1, $\bar{s}$, and η, 2 – n_1, $\bar{s}$, and curves 3 — in the n_1 direction. As the time is changed from 1 to 5 sec, there is an approximately twofold increase in the surface temperature and a decrease in the total thermal flux, and neglect of the heat flow in the $\bar{s}$ and η directions leads to large errors of their determination.

Figure 4 shows the inaccuracy in using one-dimensional and two-dimensional formulations in solving IPs for high-heat-conductivity materials of the type of copper. Taking into account the complicated nonmonotonic dependence $Q_w(\bar{s})$, the accuracy of recovering the heat flow from the solution of the three-dimensional IP can be considered to be good. At the same time, neglect of the heat flow along the circular coordinate (curve 2) and the longitudinal and circular coordinates (curve 3) leads to large errors in determining the heat flow and even to a qualitative change in its behavior. The results obtained point to the necessity of using three-dimensional algorithms for solving IPs in recovering the heat flow into a sheath from a high-heat-conductivity material.

Figure 5 illustrates the good potentialities of the proposed algorithm of solving a three-dimensional IP in recovering the surface temperature and the heat convective flux on both nonstationary and stationary portions of the body heating. Here the solution by the thin-wall method was found by the formula

$$Q_w(\bar{s}, \eta, t) = q_w(\bar{s}, \eta, t) - \varepsilon_i \sigma T_w^4 = \rho c_p L \frac{dT_w}{dt}.$$

There is a good agreement between the "exact" and numerical solutions of the three-dimensional IP. For the surface temperature, this agreement is to within graph. At the same time, the thin-wall method cannot be employed to recover heat convective fluxes in using high-heat-conductivity materials of the type of copper, since it leads to a large quantitative and qualitative disagreement with the "exact" solution.

Figure 6 shows the influence of the gas-coolant blowing on the $\bar{s}$-distribution of the stationary surface temperature $T_{w,st}$ (t = 200 sec) and the radiation equilibrium temperature $T_{w,eq}$ on the windward and leeward sides of the aerodynamic body. The radiation equilibrium temperature on the conical part of the sheath was found, as before, by

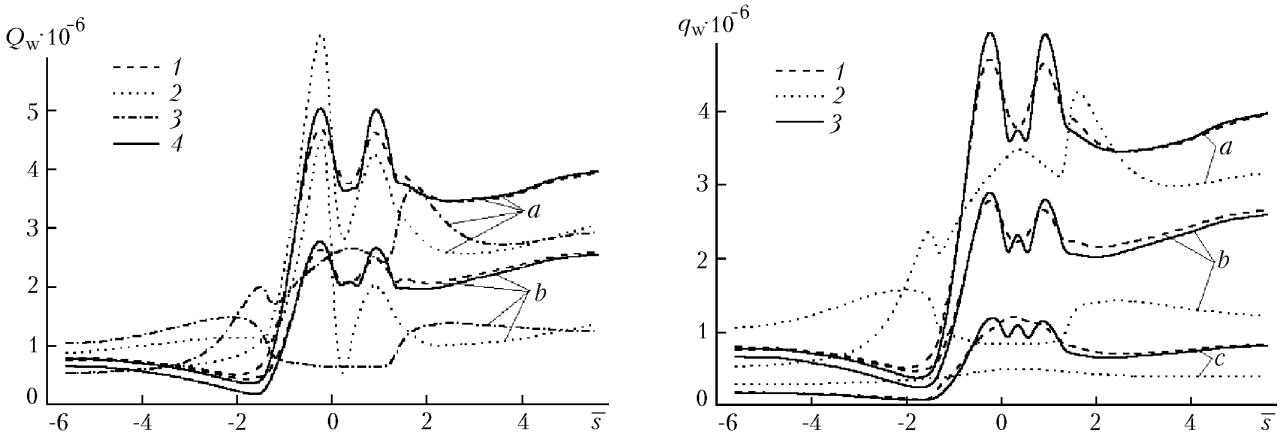

Fig. 4. Q_w distributions over $\bar{s}$ at t = 1 sec (a) and 5 sec (b) for the copper sheath obtained from the solution of the three-dimensional (1), two-dimensional (2), and one-dimensional (3) IPs; 4) "exact" solution. Q_w, W/m^2.

Fig. 5. Distributions q_w over $\bar{s}$ at t = 1 (a), 5 (b), and 200 sec (c) obtained from the solutions of the three-dimensional IP (1); by the thin-wall method (2); 3) "exact" solution. q_w, W/m^2.

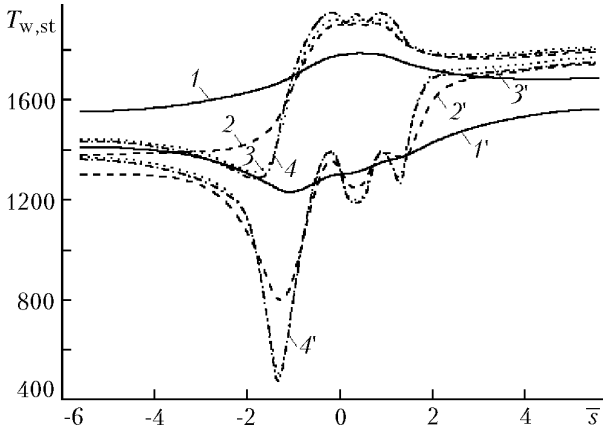

Fig. 6. Dependences of $T_{w,st}$ on $\bar{s}$ for the copper (1, 1′), steel (2, 2′), and carbon-filled plastic (3, 3′) sheaths; 4, 4′) $T_{w,eq}(\bar{s})$, 1′, 2′, 3′, 4′) with allowance for the blowing. $T_{w,st}$, K.

formula (19), and on the spherical part — from the condition of energy conservation on the surface with allowance for the stationary solution for the thin porous sheath:

$$q_w - \varepsilon\sigma T_{w,eq}^4 = (\rho v)_w \, c_{pg} \, (T_{w,eq} - T_{in}) \, .$$

From Fig. 6 it is seen that the blowing of the gas-coolant decreases the stationary temperature of the surface and the radiation equilibrium temperature. On the leeward side of the porous spherical dulling at the point of $\bar{s} \approx -1.35$, for example, the difference of the stationary values of temperatures obtained without allowance and with allowance for the blowing is about 430 K for the copper sheath, 750 K for the steel sheath, and 1020 K for the carbon-filled plastic one. And the radiation temperature values at this point differ by about 1050 K.

The sharply defined minimum in the radiation equilibrium temperature distribution is due to the fact that as the body moves at the angle of attack, the stagnation point moves to the windward side. As a result, the additional mass of the cold gas-coolant flows to the leeward side, which leads to a decrease in the thermal flow and the surface temperature. Mathematically, this shows up as an increase in the parameter b in the formula for the heat convective flux in the screen zone (17) characterizing the ratio of the total mass of the blown gas to the product of the heat-ex-

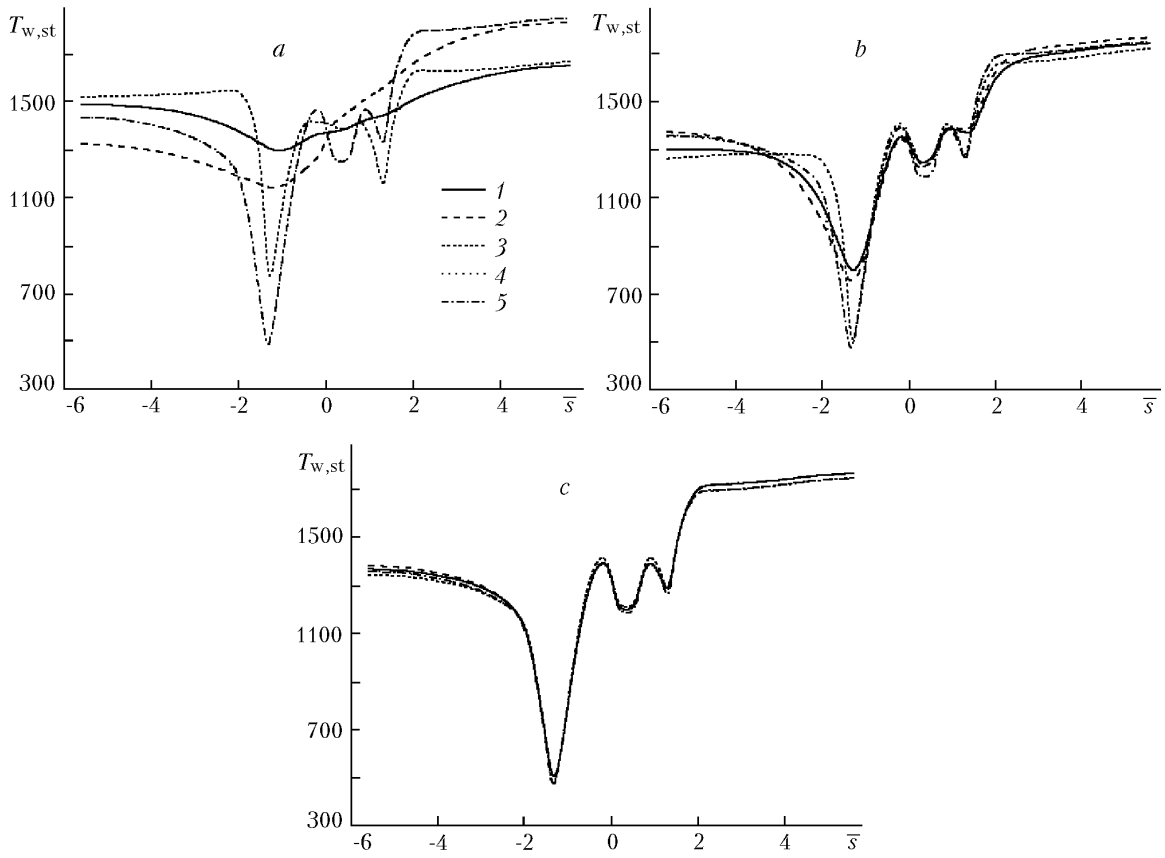

Fig. 7. Dependences of $T_{w,st}$ on $\bar{s}$ for the copper (a), steel (b), and carbon-filled plastic (c) sheaths obtained from the solution of the three-dimensional (1), two-dimensional (2, 3), and one-dimensional (4) DPs; 5) $T_{w,eq}(\bar{s})$. $T_{w,st}$, K.

change coefficient in the considered section s in the absence of blowing by the cone surface area from s_1 to the current value of s [2].

Because of the heat flow from the peripheral part of the cone into the porous nose, the temperature on the windward peripheral part of the cone decreases with increasing heat conductivity coefficient of the material λ. On the leeward peripheral part of the conical surface, $T_{w,st}$ behaves nonmonotonically depending on the heat-conductivity coefficient λ, which is due, as in the case of the absence of blowing [5], to the nonmonotonic behavior of the thermal flow along the circular coordinate η and the heat flow in the circular direction. On the porous spherical part in the vicinity of the front critical point, where the laminar flow in the boundary layer is realized, an increase in the heat-conductivity coefficient λ is followed by an increase in the stationary surface temperature.

Because of the heat flow along the longitudinal and circular coordinates, the stationary surface temperature on the peripheral part of the cone for the copper sheath on the windward side is about 200 K lower than for the steel and carbon-filled plastic sheaths. On the peripheral part of the cone on the leeward side the increase in this temperature is somewhat smaller.

Figure 7 shows the influence of the thermophysical properties of the sheath material on the stationary surface temperature distributions on the longitudinal coordinate. Here curves 1 were obtained with allowance for the heat transfer on n_1, $\bar{s}$, and η, curves 2 — on n_1 and $\bar{s}$, curves 3 — on n_1 and η, and curves 4 — on n_1. The radiation equilibrium temperature 5 coincided to within graph with the stationary surface temperature 4, which is one of the confirmations of the reliability of the calculations. Analysis of the results presented shows that the influence of the heat flow on the stationary surface temperature distribution for the carbon-filled plastic sheath is practically absent and the influence of the heat flow for the steel sheath is immaterial everywhere, except for the point of $\bar{s} \approx -1.48$, where the difference is about 100–150 K. And it is very essential to take into account the heat flow in all directions for the copper sheath, where the difference is a few hundred degrees.

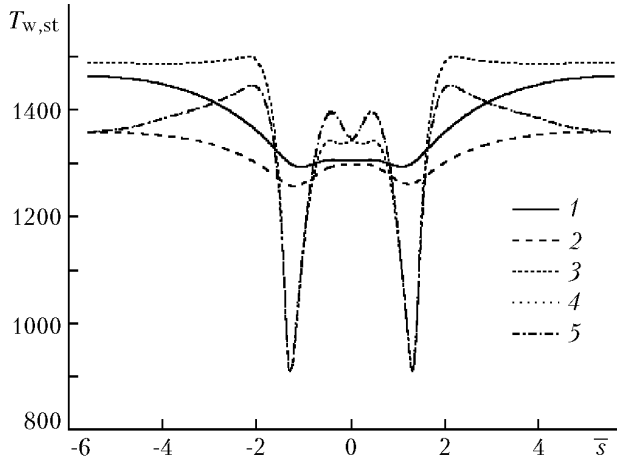

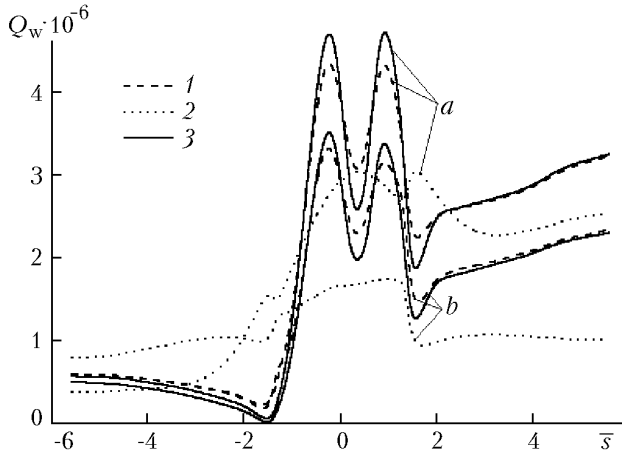

Fig. 8. Dependences of $T_{w,st}$ on $\bar{s}$ for the copper sheath in the $\eta = \pi/2$ and $\eta = 3\pi/2$ planes obtained from the solution of the three-dimensional (1), two-dimensional (2, 3), and one-dimensional (4) DPs; 5) $T_{w,eq}(\bar{s})$. $T_{w,st}$, K.

Fig. 9. Q_w distributions over $\bar{s}$ at t = 1 (a) and 5 sec (b) obtained from the solution of the three-dimensional IP (1) and by the thin-wall method (2); 3) "exact" solution. Q_w, W/m^2.

Figure 8 gives the stationary surface temperature distributions for the copper sheath on the longitudinal coordinate in the planes of $\eta = \pi/2$ and $\eta = 3\pi/2$. From comparison of these figures it follows that in the planes of $\eta = \pi/2$ and $\eta = 3\pi/2$ compared to the planes of $\eta = 0$ and $\eta = \pi$ the temperature decreases on the windward side and increases on the leeward side, and the temperature profiles are symmetric about the point of $\bar{s} = 0$.

And, finally, Figure 9 illustrates the inexpediency of using the thin-wall method to recover the thermal flow Q_w into a sheath made of a high-heat-conductivity material in the presence of blowing. Here the solution by the thin-wall method was found by the formula

$$Q_w(\bar{s}, \eta, t) = q_w(\bar{s}, \eta, t) - \varepsilon\sigma T_w^4 = \rho c_p L \frac{dT_w}{dt} + (\rho v)_w c_{pg} (T_w - T_g) .$$

As a result of the numerical calculations, it has been shown that the proposed three-dimensional algorithm for solving IPs is stable to perturbations of the input temperature $T_{ins}^{exp}(s, \eta, t)$ and permits recovering heat convective flows in a wide range with allowance for the gas-coolant blowing.

CONCLUSIONS

Using the proposed algorithms of solving three-dimensional direct and inverse heat-exchange problems, we have investigated the influence of the heat flow along the longitudinal and circular coordinates and the gas-coolant blowing on the characteristics of the spatial heat exchange. The effectiveness of simultaneous use of high-heat-conductivity materials and gas-coolant blowing in order to lower the maximum temperatures on thermally stressed parts of the surface of the aerodynamic body has been shown. The error of recovery of the heat-exchange characteristics on the surface of high-heat-conductivity materials has been determined by means of the one- and two-dimensional algorithms for solving direct and inverse problems and the thin-wall method.

NOTATION

t, time, sec; r and z, transverse and longitudinal components of the cylindrical coordinate system; n_1, s, η, components of the natural coordinate system; T, temperature, K; p, pressure, Pa; ρ, density, kg/m^3; $(\rho v)_w$, gas-coolant flow in pores, kg/(m^2·sec); c_p, heat-capacity coefficient, J/(kg·K); λ, heat-conductivity coefficient, W/(m·K); h_r, recovery enthalpy, J/kg; h_w, gas enthalpy on the wall, J/kg; h_{e0}, gas enthalpy at the outer boundary of the boundary layer

at the stagnation point, J/kg; H, r_1, r_2, Lamé coefficients; $\bar{r}_{2w}$, dimensionless Lamé coefficient on the outer surface of the conical part of the body; α, heat-transfer coefficient, W/(m^2·K); R_N, spherical dulling radius, m; φ, porosity; $\bar{s}$, dimensionless longitudinal coordinate; σ, Stefan–Boltzmann constant, W/(m^2·K^4); ε_i (i = 1, 2), radiating capacity of the surface of the aerodynamic material; q_w, heat convective flow from the gaseous phase, W/m^2; Q_w, total heat flow into a solid body, W/m^2; β and θ, angle of attack and cone angle, deg; Pr, Prandtl number; γ, adiabatic exponent; L, sheath thickness, m; V_∞, ρ_∞, and M_∞, rate of motion, density, and Mach number in the incident flow, m/sec, kg/m^3; u_e, velocity of gas at the outer boundary of the boundary layer, m/sec; v_m, maximum velocity of gas, m/sec; T_{ins}^{exp}, temperature on the inner surface of the body sheath, which is the initial "experimental" temperature in solving the inverse problem; $\tilde{s}$, dimensionless longitudinal coordinate in the coordinate system with origin at the stagnation point O_1; $\tilde{s}_*$, coordinate of the laminar-turbulent transition point in the coordinate system with origin at the stagnation point; b, parameter in the formula for the heat convective flow in the screening zone (17); ζ_1, ζ_2, approximation parameters in the formula for the heat flow in the screening zone (17); b_1, b_2, approximation parameters in the formula for the heat capacity of gas c_{pg}. Subscripts: ∞, incident flow; e, outer boundary of the boundary layer; e0, outer boundary of the boundary layer at the stagnation point; w, gas-solid interface; ins, inner surface of the sheath; r, recovery; exp, experiment; 1, 2, numbers of regions of the composite sheath; g, gas in the porous medium; in, fin, *, m and Σ, initial, final, characteristic, maximum, and total values of quantities; overscribed bar, for dimensionless quantities; (0), for heat-exchange parameters (α/c_p), q_w, in the absence of blowing; st, for stationary temperature; eq, for radiation equilibrium temperature.

REFERENCES

1. V. I. Zinchenko, A. G. Kataev, and A. S. Yakimov, *Prikl. Mekh. Tekh. Fiz.*, **23**, No. 6, 57–64 (1992).
2. V. I. Zinchenko, V. I. Laeva, and T. S. Sandrykina, *Prikl. Mekh. Tekh. Fiz.*, **37**, No. 5, 106–114 (1996).
3. V. I. Zinchenko and A. S. Yakimov, *Prikl. Mekh. Tekh. Fiz.*, **40**, No. 4, 162–169.
4. V. I. Zinchenko and A. Ya. Kuzin, *Prikl. Mekh. Tekh. Fiz.*, **40**, No. 5, 123–132 (1999).
5. V. I. Zinchenko and A. Ya. Kuzin, *Prikl. Mekh. Tekh. Fiz.*, **43**, No. 1, 144–152 (2002).
6. V. I. Zinchenko and A. Ya. Kuzin, *Prikl. Mekh. Tekh. Fiz.*, **43**, No. 5, 87–96 (2002).
7. O. M. Alifanov, in: *Proc. IV Minsk Int. Forum "Heat and Mass Transfer–MIF-2000"* [in Russian], Vol. 3, 22–26 May 2000, Minsk (2000), pp. 3–13.
8. O. M. Alifanov and A. V. Nenarokomov, *Dokl. Ross. Akad. Nauk*, **325**, No. 5, 950–954 (1992).
9. O. M. Alifanov and A. V. Nenarokomov, *Teplofiz. Vys. Temp.*, **37**, No. 2, 231–238 (1999).
10. A. Ya. Kuzin, in: *Selected Papers presented at Int. Conf. "Conjugate Problems of Mechanics and Ecology"* [in Russian], Tomsk (2000), pp. 190–205.
11. B. A. Zemlyanskii and G. N. Stepanov, *Izv. Akad. Nauk SSSR, Mekh. Zhidk. Gaza*, No. 5, 173–177 (1981).
12. Yu. V. Polezhaev and F. B. Yurevich, *Thermal Protection* [in Russian], Moscow (1976).
13. V. N. Kharchenko, *Teplofiz. Vys. Temp.*, No. 1, 101–105 (1972).
14. N. N. Yanenko, *Subincremental Method of Solution of Multidimensional Problems of Mathematical Physics* [in Russian], Novosibirsk (1967).
15. A. M. Grishin, A. Ya. Kuzin, V. L. Mikov, et al., *Solution of Some Inverse Problems of the Mechanics of Reacting Media* [in Russian], Tomsk (1987).
16. A. A. Samarskii and E. S. Nikolaev, *Methods of Solution of Grid Equations* [in Russian], Moscow (1978).
17. O. M. Alifanov, V. K. Zantsev, B. M. Pankratov, et al., *Algorithms of the Diagnostics of Thermal Loads of Flying Vehicles* [in Russian], Moscow (1983).
18. Yu. S. Zav'yalov, B. I. Kvasov, and V. L. Miroshnichenko, *Methods of Spline-Functions* [in Russian], Moscow (1980).
19. A. Ya. Kuzin and N. A. Yaroslavtsev, Use of regulating algorithms for solution of a non-linear boundary-value problem of heat conduction, Dep. at VINITI on 22.07.87, No. 5280, Moscow (1987).
20. V. A. Antonov, V. D. Gol'din, and F. M. Pakhomov, *Aerodynamics of Bodies with Blowing* [in Russian], Tomsk (1990).